nature research

https://doi.org/10.1038/s41592-020-0933-6

Supplementary information

Feature-based molecular networking in the GNPS analysis environment

In the format provided by the authors and unedited

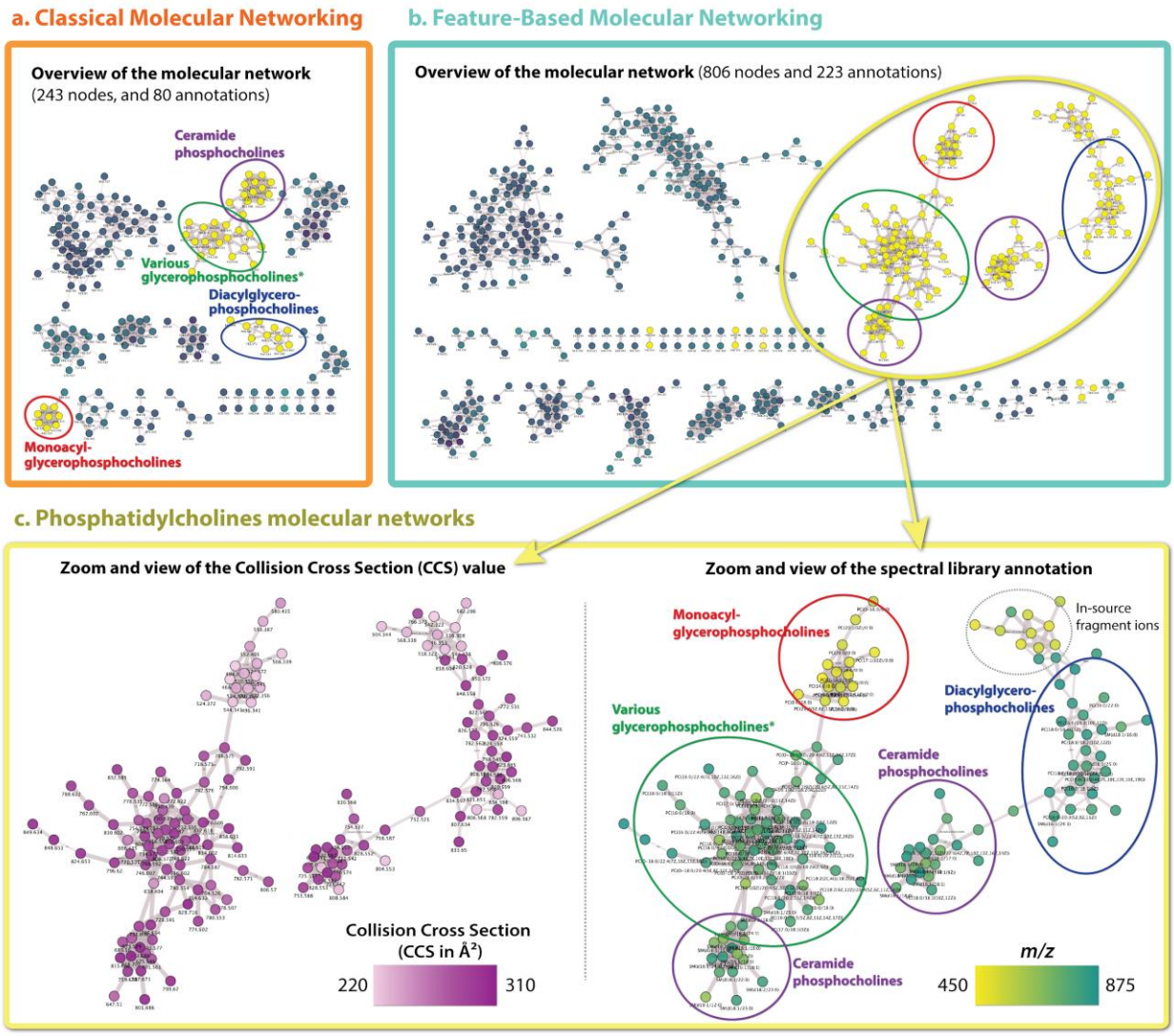

Supplementary Figure 1. Analysis of trapped ion mobility spectrometry (TIMS) data of the reference serum sample (NIST 1950 SRM) processed used with Feature-Based Molecular Networking (FBMN) on GNPS. The data were collected on a tims-TOF Pro (Bruker Daltonics, Bremen) in Parallel-Accumulation Serial Fragmentation (PASEF) mode, and processed with MetaboScape. (a) Molecular networks obtained with classical molecular networking; (b) molecular networks obtained with FBMN; and (c) views of the phosphatidylcholine molecular networks with FBMN (the node color gradient to the left shows the cross-collision section value, and the *m/z* value to the right). Results showed that the use of classical molecular networking drastically reduces the number of nodes (-70%) and spectral annotations (-65%) compared to FBMN. This can be explained by the fact that many isomers are present amongst the lipids annotated (mostly phosphatidylcholines). These isomers tend to produce similar MS^2 spectra which can be merged by MS-Cluster when performing classical molecular networking. FBMN ensures that the "LC-TIMS-MS" features detected by MetaboScape are preserved which enables the visualization of the Collision Cross Section value in the molecular networks.

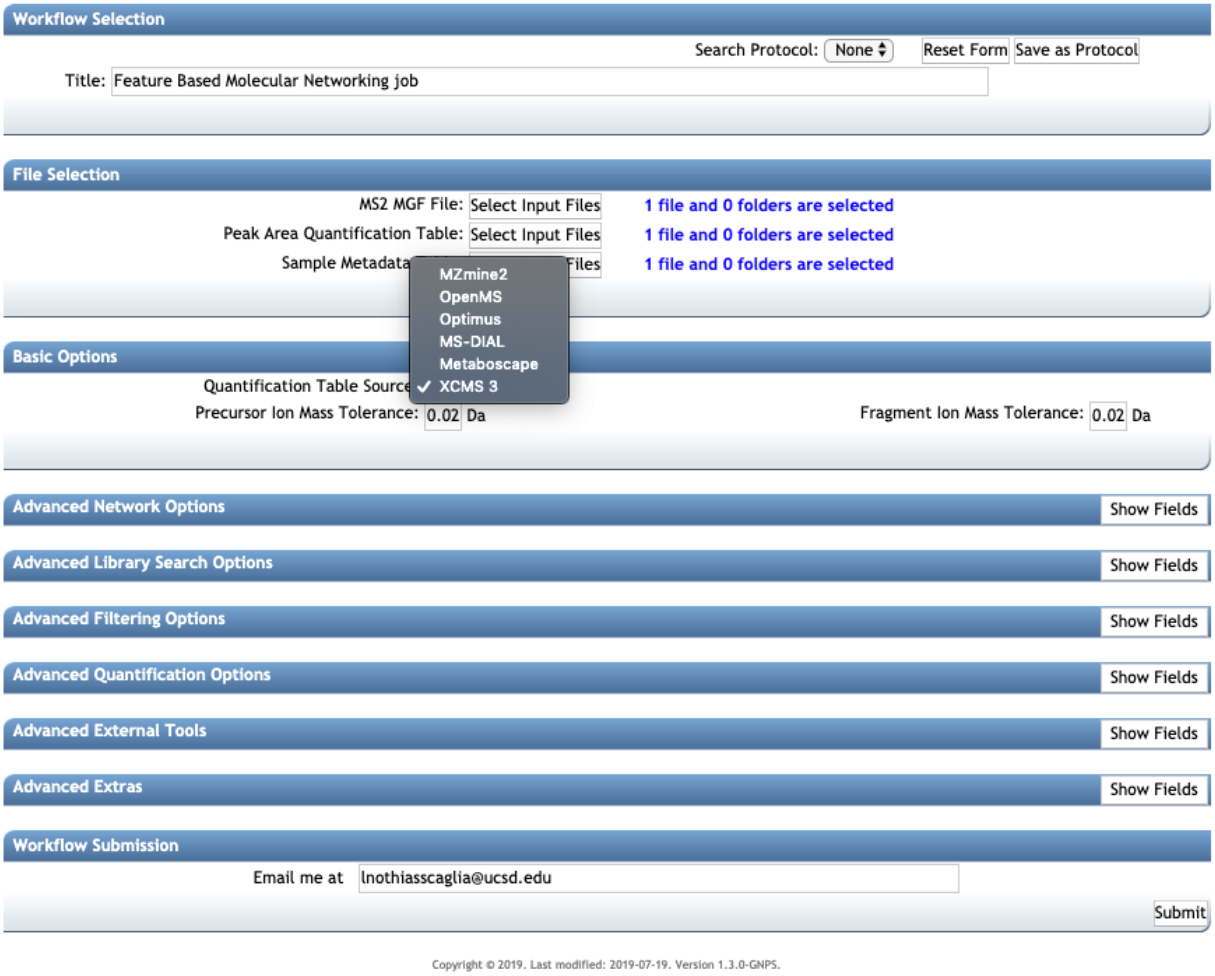

Supplementary Figure 2. Feature-based molecular networking workflow standard interface on GNPS (https://gnps.ucsd.edu).

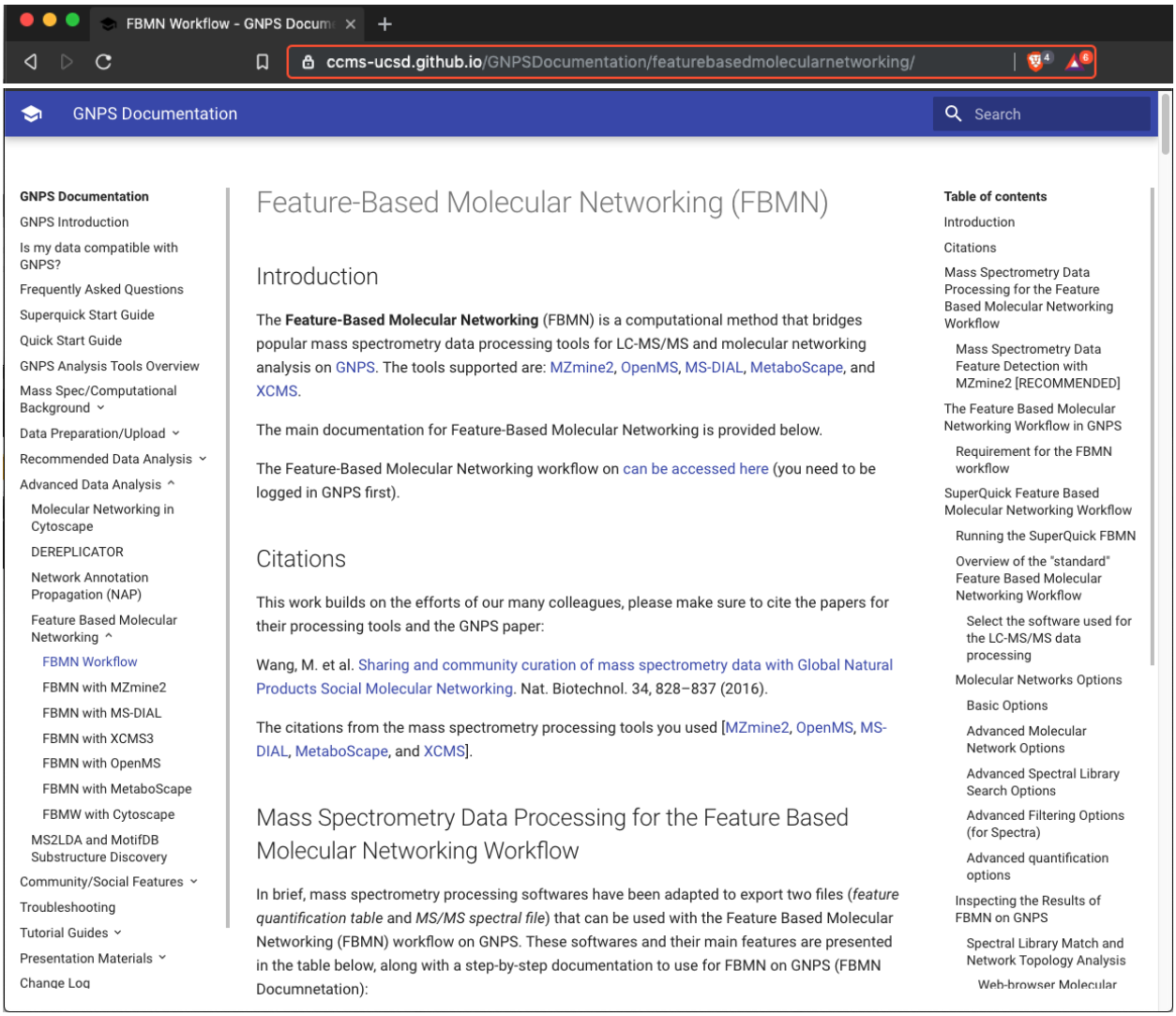

Supplementary Figure 3. The feature-based molecular networking documentation on GNPS (**https://ccms-ucsd.github.io/GNPSDocumentation/featurebasedmolecularnetworking/**).

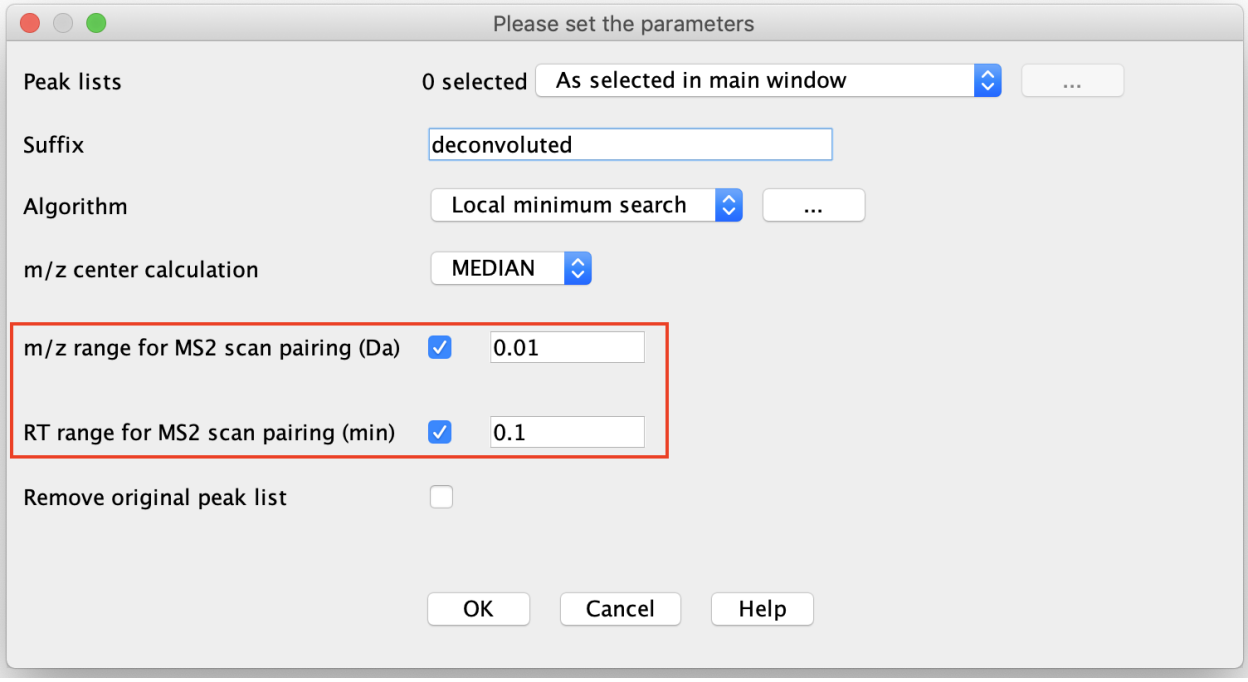

Supplementary Figure 4. The *Chromatogram deconvolution* module in MZmine and the options added for the pairing of MS^1 feature and MS^2 scans available since MZmine 2.27.

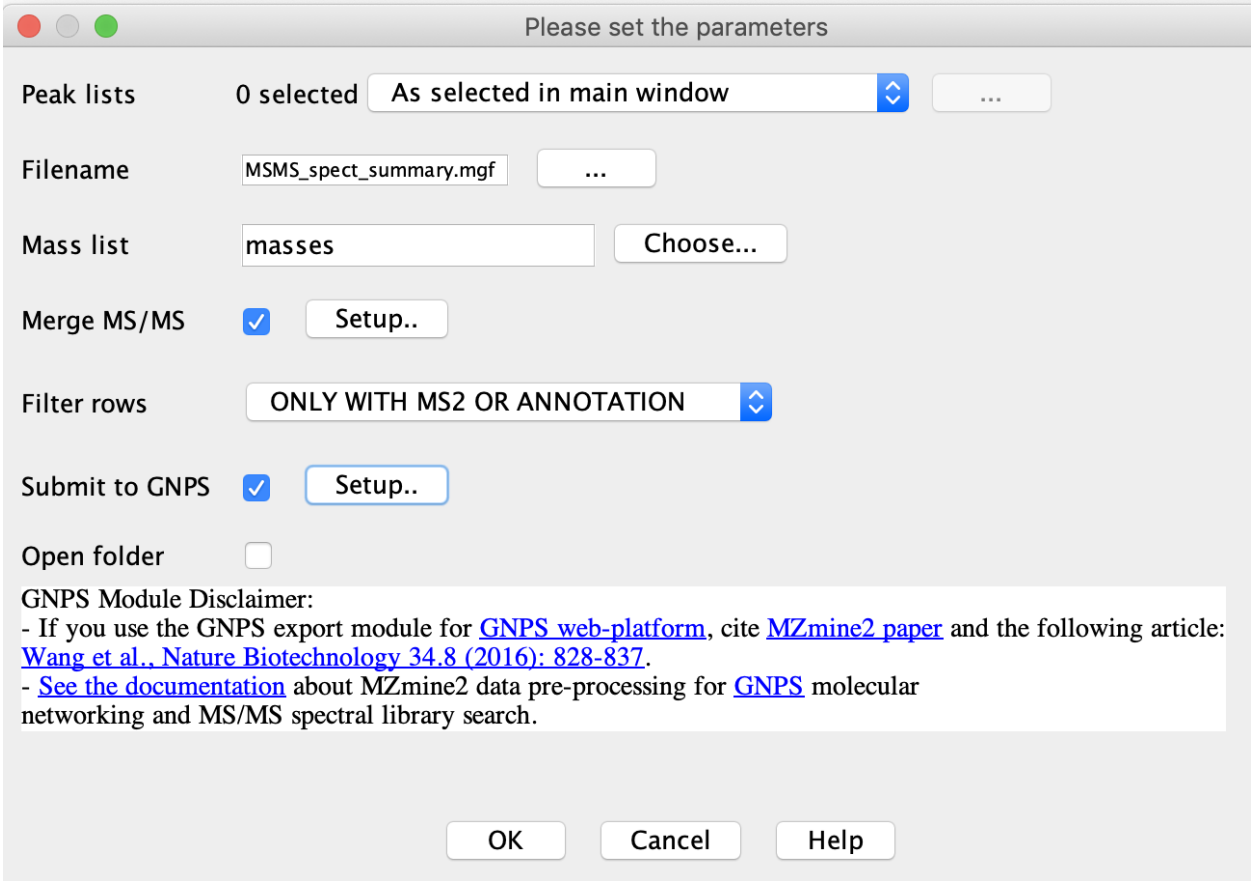

Supplementary Figure 5. The *Export for/Submit to GNPS* module interface in MZmine, available since version MZmine 2.37.

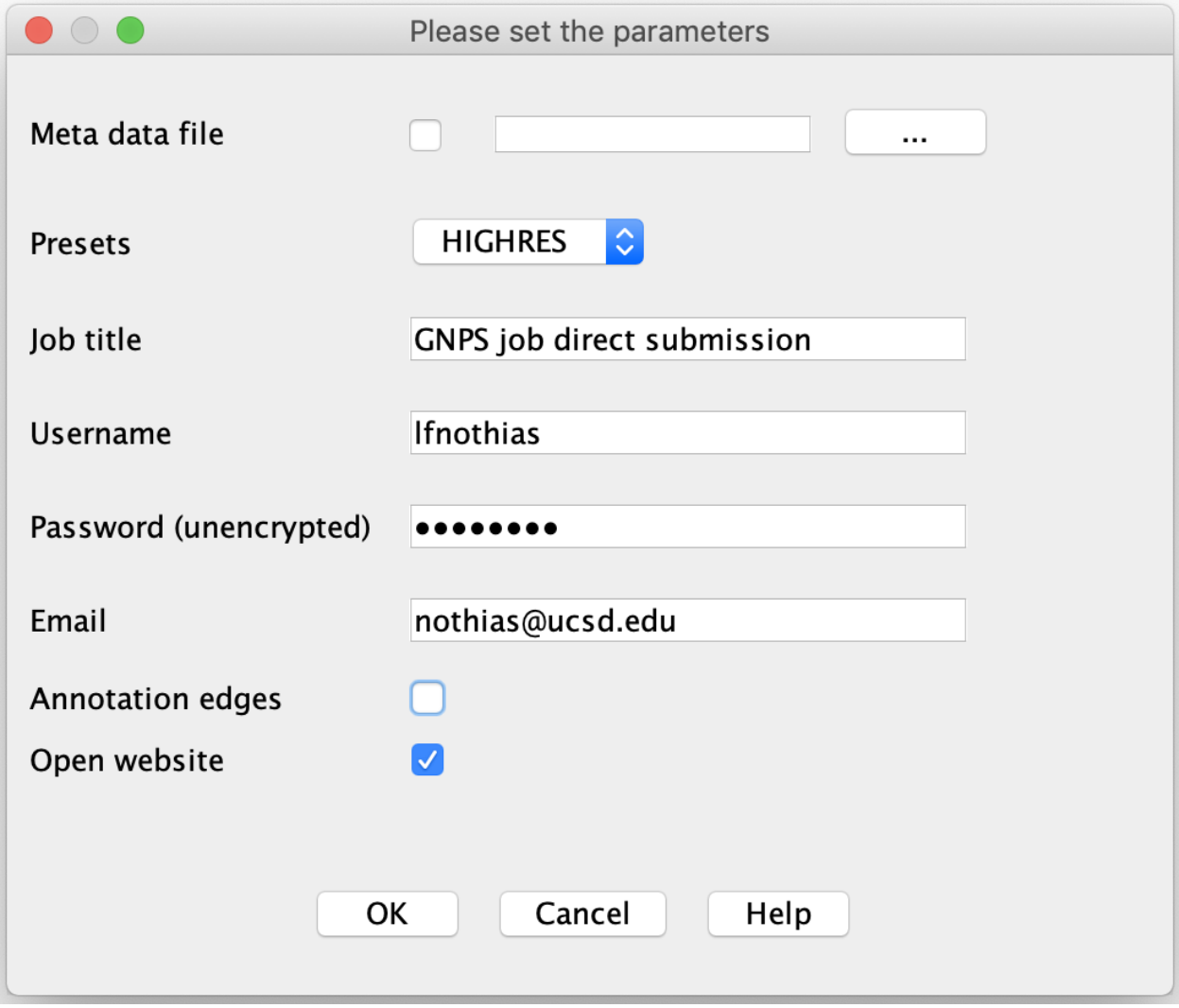

Supplementary Figure 6. Direct submission to GNPS with the *Export for/Submit to GNPS* module in MZmine.

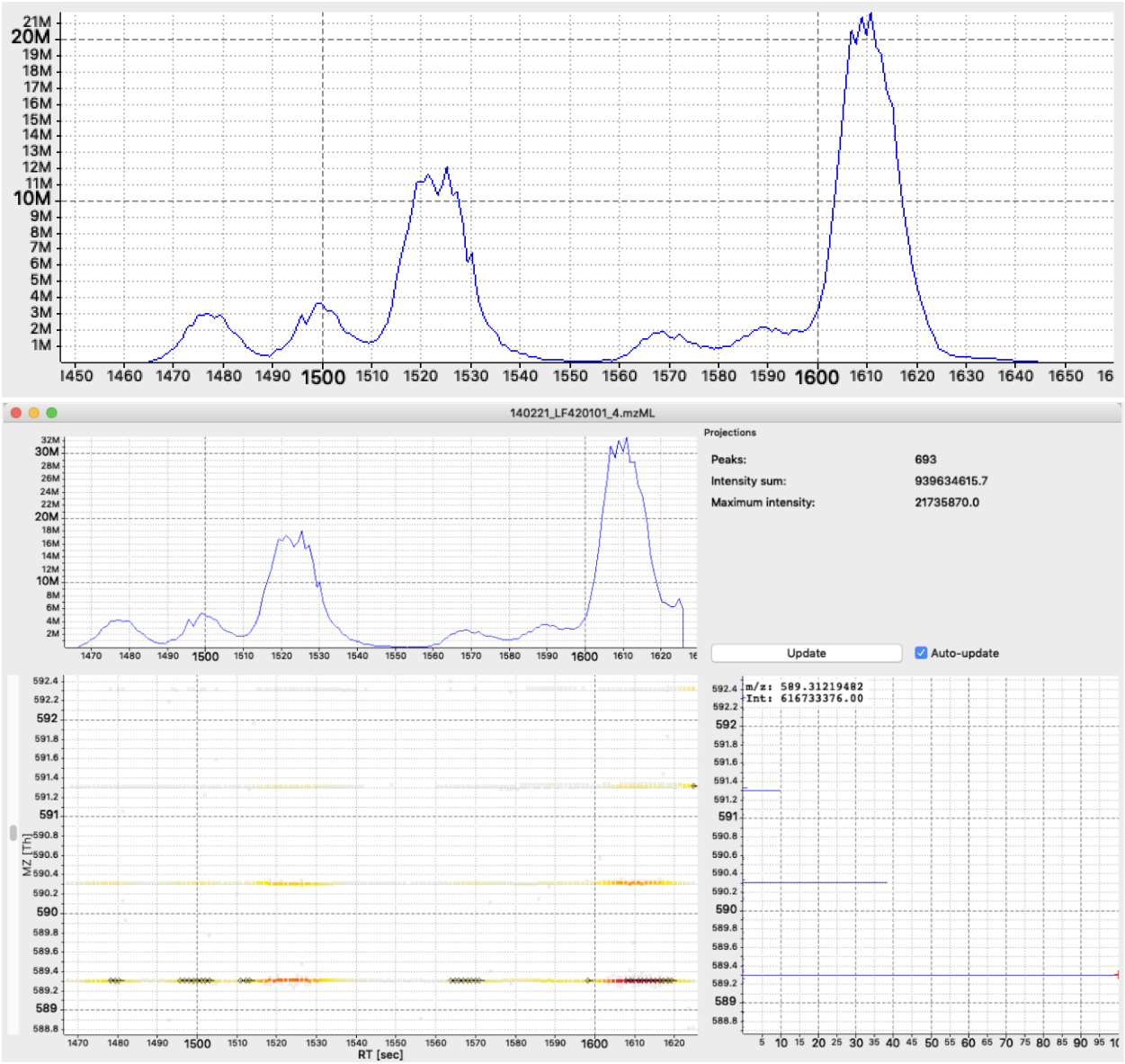

Supplementary Figure 7. Screenshots from OpenMS TOPPView. Top: Extraction Ion Chromatogram (EIC) of *m/z* 589.31 for the *Euphorbia dendroides* extract (LF420101_4.mzML, n = 1 LC-MS^2 experiment) in the range 1450-1650 seconds. Bottom: Two dimensional LC-MS view of the compounds the isotopic pattern for the *m/z* 589.31 for the extract of *Euphorbia dendroides*. The top panel shows the EIC for the range *m/z* 589-592 and 1470-1640 seconds. The lower left panel shows the different intensities per *m/z* values, and the presence of fragmentation scans (black dots). The right panel shows the full spectrum for the range.

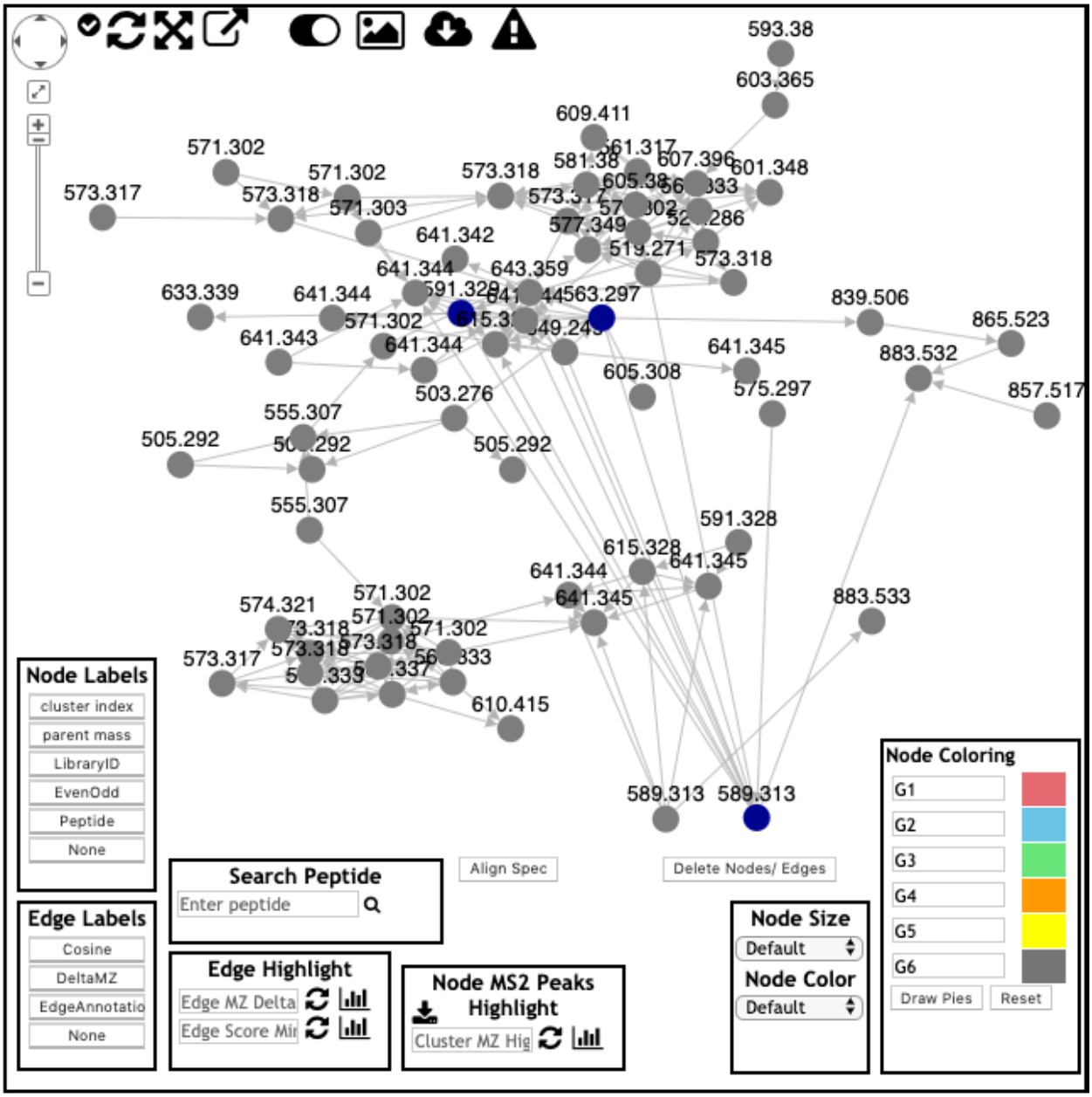

Supplementary Figure 8. Classical molecular networking analysis of *Euphorbia dendroides* dataset. View of the deoxyphorbol ester molecular network.

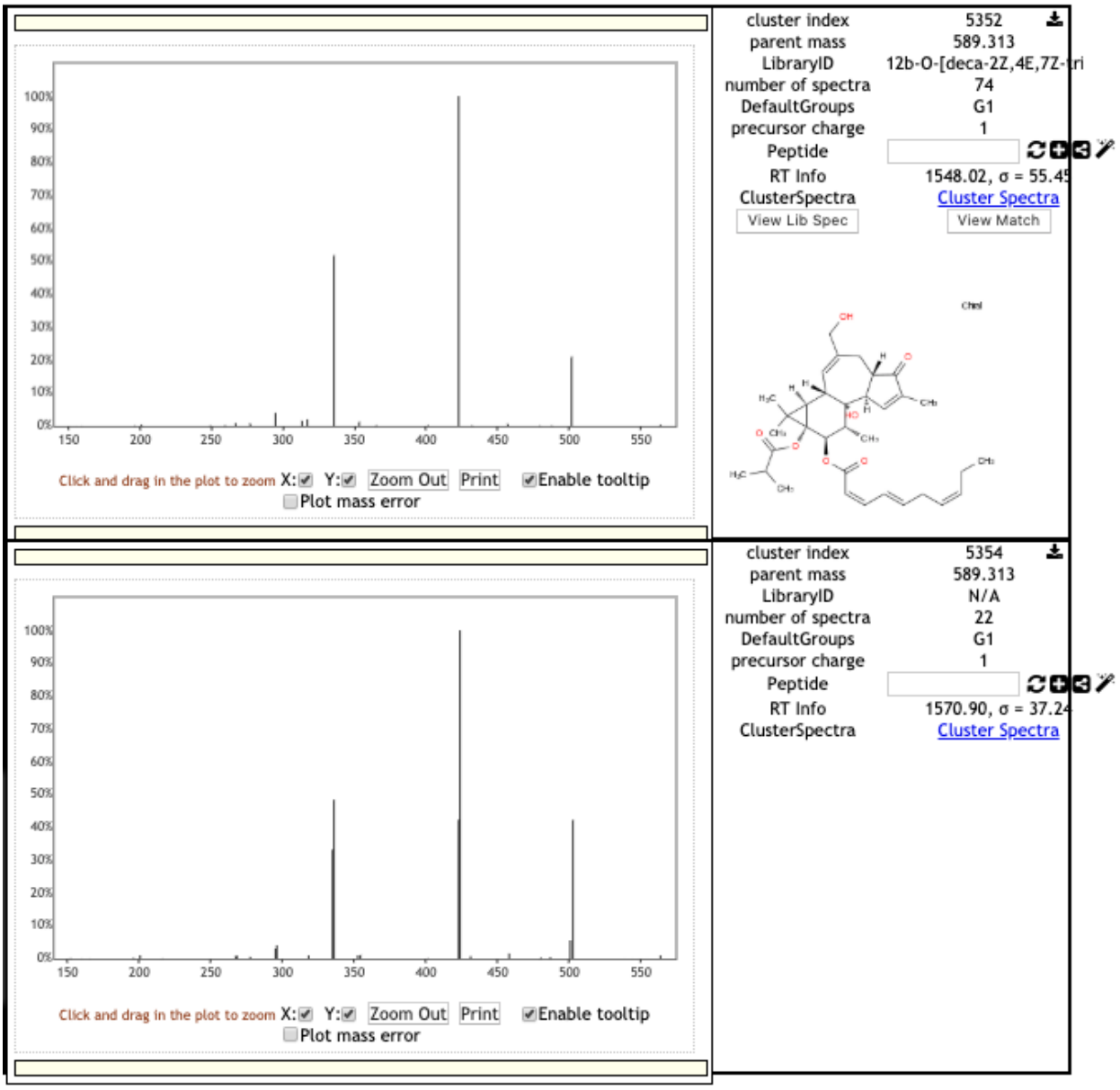

Supplementary Figure 9. Classical molecular networking analysis of *Euphorbia dendroides* dataset (n = 1 LC-MS^2 experiment per sample). View of the MS^2 spectra for the two at *m/z* 589.313 nodes.

a MS² of *m/z* 589.31 (scan = 2922, ret. time = 1497 sec)

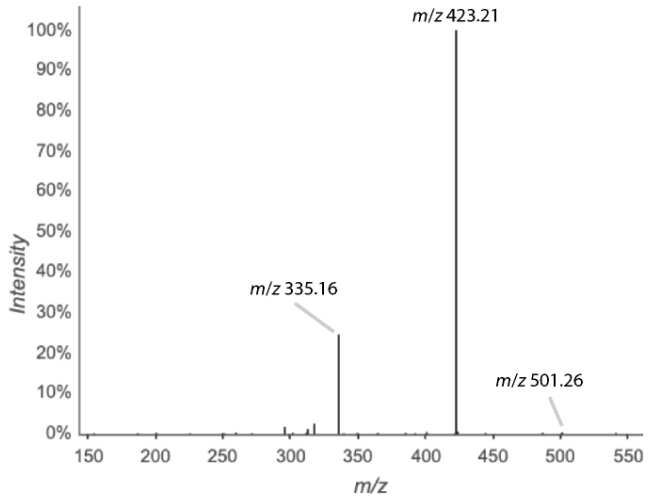

b MS² of *m/z* 589.31 (scan = 3060, ret. time = 1565 sec)

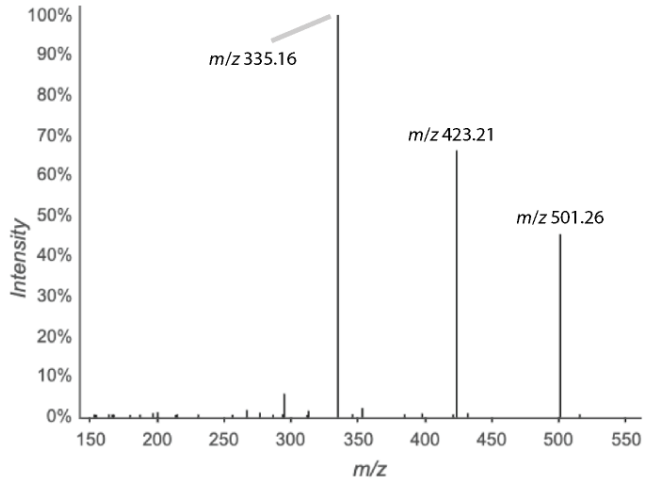

c MS² of *m/z* 589.31 (scan = 3164, ret. time = 1616 sec)

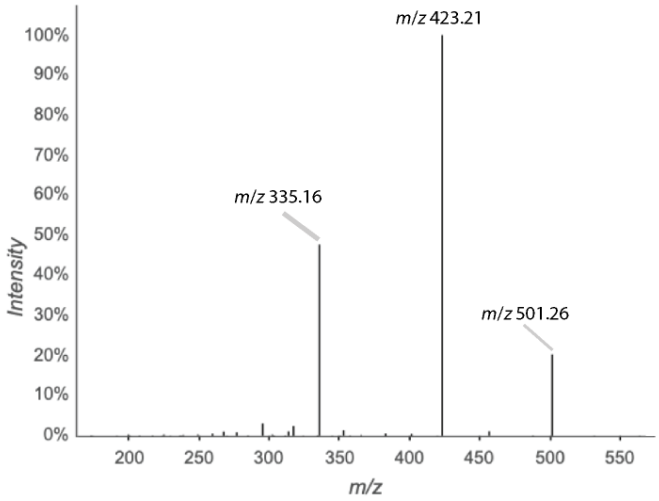

Supplementary Figure 10. Different MS^2 spectra for the ion *m/z* 589.31 observed in the *E. dendroides* extract (n = 1 LC-MS^2 experiment per sample). (a) The first spectral type was observed for the peaks at 24.6 - 25.2 min and characterized by a base peak at *m/z* 423.21 and a fragment ion *m/z* 335.16 with 20% relative intensity. (b) The second spectral type was observed for peaks at 26.1 min and a base peak at *m/z* 335.16, and fragment ions *m/z* 423.21 and 501.26 with 70-80% and 50-60% of relative intensities, respectively. (c) The third population was found for the chromatographic peaks at 26.1 - 27.0 min with a base peak at *m/z* 423.21 and fragment ions *m/z* 335.16 and 501.26 with 35-45% and 15-25% of relative intensities, respectively.

Supplementary Note 1: Detailed discussion about the differences observed between classical molecular networking vs FBMN methods for *Euphorbia dendroides* data.

A comparison of results between classical molecular networking vs FBMN (with MZmine) for the *Euphorbia dendroides* dataset is presented in Supplementary Table 1. FBMN is heavily dependent upon user-defined parameters selected during all steps of processing, including peak picking, chromatogram building and deconvolution, isotope grouping, feature alignment and gap filling. The discussion here described differences between the results obtained with classical and FBMN. For the *E. dendroides* dataset processed in MZmine with parameters described in the method, we observed that classical molecular networking produced more network nodes than FBMN. However, FBMN offered a higher spectral annotation rate (5.23%) than classical molecular networking (2.16% with a minimum cluster size = 2). The ratio between unique annotations/total annotations showed that FBMN is capable of separating different isomers, which get merged into one spectrum through the MS-Cluster algorithm in the classical molecular networking workflow (0.42 instead of 0.78 for classical molecular networking). However FBMN was found to provide less unique annotations than classical molecular networking (17 versus 22). This may indicate that relevant features were filtered out during MZmine processing for the FBMN using selected parameters.

MZmine offers various heuristic filters that can be used to reduce the number of features detected. We investigated the results of these filters on the network topology and annotation. When the filters “minimum 2 isotopes detected” and “minimum 2 occurrences” were used for FBMN analysis, the number of nodes became 315 nodes instead of 765 when no filter is used. Moreover, these two filters decreased the proportion of single nodes (31.4% instead of 44.8%), and increased the spectral annotation rate (10.47% instead of 5.23%) which suggests that they efficiently removed low quality spectra. Nevertheless, the use of these filters in MZmine decreased the number of nodes in the molecular network analysis, as seen in the deoxyphorbol molecular family (19 versus 39 nodes without filters). This can be explained by the nature of this dataset, which contains unique spectra from fractions of an *E. dendroides* extract, likely exhibiting high chemical diversity with many unique compounds. Thus, the use of the “minimum 2 occurrences" filter in MZmine, is filtering them out. In addition, the use of the filter “2 minimum isotopes detected” will filter out features that were detected at the limit of detection, and for which no C_{13} isotopic peak can be observed/paired.

As different parameters selected during MZmine processing affect the final outcome, also the use of different processing software might influence results retrieved. The present FBMN results with MZmine enabled the discrimination of more isomers for the ion *m/z* 589.311, than when OpenMS was used in the original paper[1], which illustrates how different processing software could lead to different results based on the parameters used and their specificities. In the present case, when using the OpenMS *FeatureFinderMetabo* algorithm, it was observed that closely eluting isomeric features were often detected as a single feature instead of multiple, despite trying various parameters designed to separate features such as the trace_termination_criteria (*outlier*, *sample_rate*)."

Supplementary Table 1. Results for classical molecular networking and feature-based molecular networking (with MZmine) for the *Euphorbia dendroides* dataset.

	Number of nodes	**Single nodes**	**Unique library annotations**	**Total library annotations**	**Spectral annotation rate**	**Size of the deoxyphorbol ester network**
Classical molecular networking (minimum cluster size = 2, default)	1,297	519 (40.0%)	22	28	2.16 %	22 (538 total spectra)
Feature based molecular networking without feature filters	765	342 (44.7%)	17	40	5.23 %	39
Feature based molecular networking with feature filter ("minimum 2 isotopes detected", "minimum 2 occurrences")	315	98 (31.1%)	15	33	10.47%	19

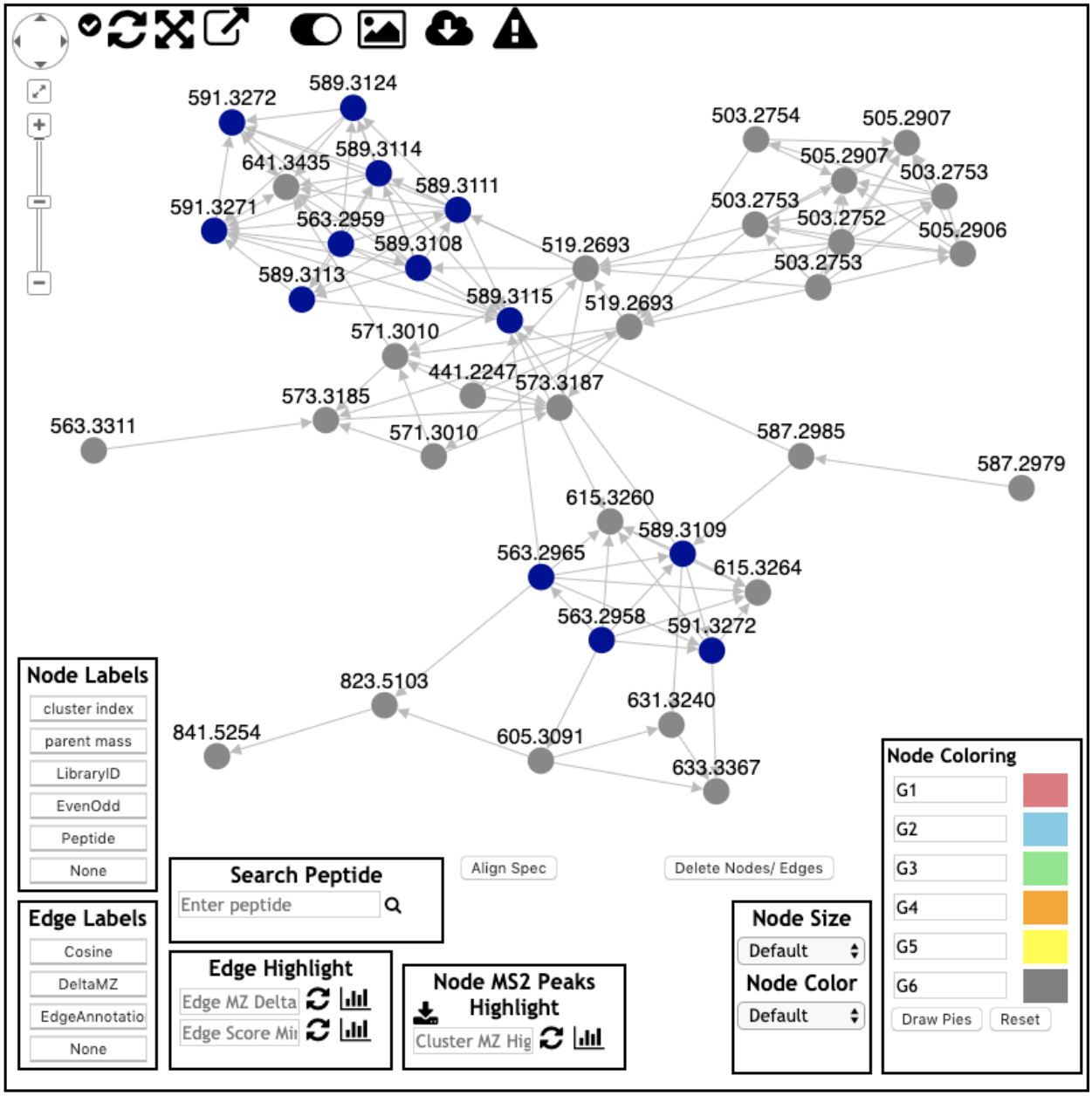

Supplementary Figure 11. Results of [feature-based molecular networking] with MZmine for the *E. dendroides* datasets (n = 1 LC-MS^2 experiment per sample). View of the entire deoxyphorbol cluster molecular network.

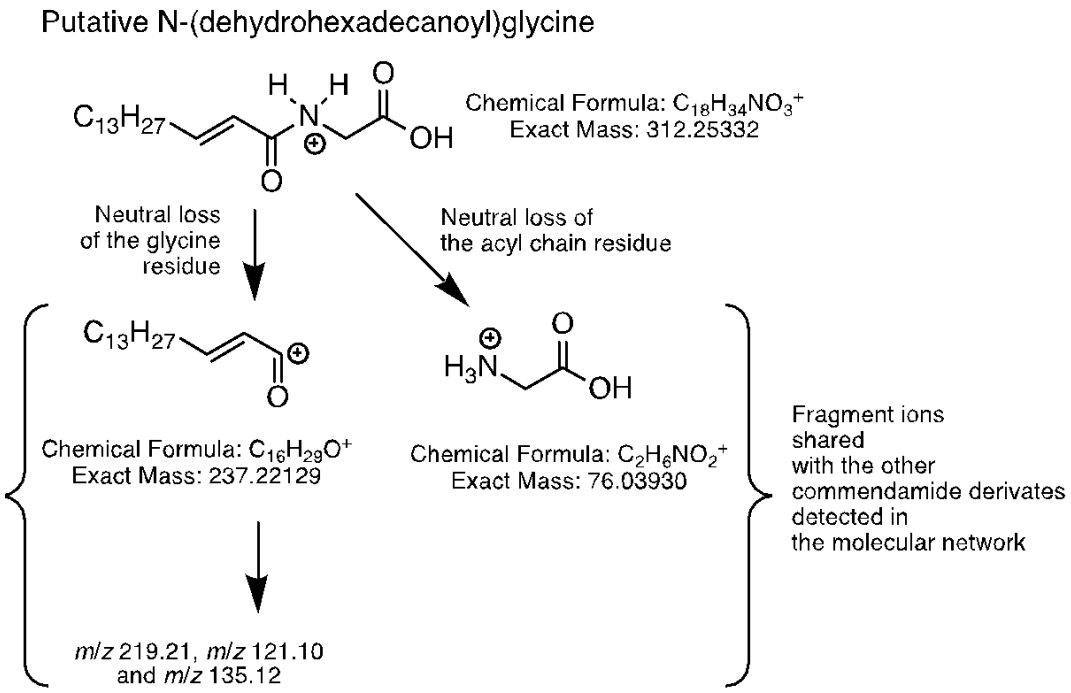

Supplementary Figure 12. Annotation of (dehydrohexadecanoyl)glycine, a putative commendamide derivative in the American Gut Project dataset (dehydrohexadecanoyl)glycine using FBMN on GNPS.

Supplementary Note 2: Protocol for the MassIVE MSV00008263 **dataset (EDTA case).**

Sample preparation. The 96-well plate PhreeTM Phospholipid Removal Kit was rinsed with 300 μL of MeOH (100%) and centrifuged at 500 g for 5 min, three times prior to sample addition. Blood plasma was stored at -80°C prior to extraction. The plasma microtubes were thawed at room temperature prior to extraction. Plasma samples were placed randomly into one of two PhreeTM Phospholipid Removal Kit 96-well plates. The thawed plasma samples were vortexed for 5 s and centrifuged for 1 min @ 5000 rpm prior to pipetting 50 µL of each sample into the 96-well PhreeTM Phospholipid Removal Kit. 200 µL of MeOH (100%) with 500 ng mL-1 lithocholic acid - d4 as an internal standard was added to each sample well using a multichannel pipette; the solution was aspirated and dispensed five times to mix plasma and organic solvent. 250 µL of a mixture of the bile acid standards at a concentration of 1000 ng mL-1, individually, in MeOH-Water (4:1) was added to 3 separate well (split 2 on one SPE plate and 1 on the other). A 96-well plate (Eppendorf® Microplate 96/U-PP) was placed under the PhreeTM Phospholipid Removal Kit to collect the sample, and centrifuged at 500 g for 5 min. The PhreeTM Phospholipid Removal Kit portion was discarded and the sample-containing 96-well plate was evaporated until dry using a CentriVap Benchtop Vacuum Concentrator (Labconco, Kansas City, MO, USA). The 96-well plate containing the dried extract were covered (Storage Mat IIITM 3080) and stored at -80°C prior to analysis. Immediately prior to analysis,

the dried extract material was resuspended in 250 µL of MeOH-water (1:1) with 250 ng mL-1 cholic acid - d4, sonicated for 5 min, centrifuged for 5 min at 500 g, and covered with a plate sealing film (Zone-FreeTM Sealing Films).

Data acquisition. Plasma metabolite extracts were analyzed using an ultra-high performance liquid chromatography device (Vanquish, Thermo Fisher Scientific, MA, USA) coupled with an Orbitrap mass spectrometer (Q Exactive, Thermo Fisher Scientific, MA, USA). Chromatographic separation was carried out using a Kinetix C18 1.7 µm, 100 Å, 50 x 2.1 mm column with corresponding C18 guard cartridge maintained at 40°C during separation. 5.0 µL of extract was injected per sample. Mobile phase composition was as follows: A, water with 0.1% formic acid (v/v) and B, acetonitrile with 0.1% formic acid (v/v). Gradient elution was performed as follows: 0.0, 5.0% B; 1.0, 5.0% B; 1.1, 25.0% B; 5.0, 60.0% B; 5.75, 100.0% B; 6.5, 100%; 6.6, 5.0% B; 7.0, 5.0% B. Flow rate of 0.5 mL min-1 was held constant. Heated electrospray ionization (HESI) was performed in positive ion mode using the following source parameters: spray voltage, 3500 V; capillary temperature, 380 °C, sheath gas, 60.00 (a.u.); auxiliary gas, 20.00 (a.u.); sweep gas, 3.00 (a.u); probe temperature, 300 °C; and S-lens RF level, 60. The data-dependent acquisition parameters were set as follows: MS1 scans were collected at 30,000 resolution from m/z 150 to 1500 (~7 Hz) with a maximum injection time of 100 ms, 1 microscan, and an automatic gain control target of $1x10^6$. The top 3 most abundant precursor ions in the MS1 scan were selected for fragmentation with an m/z isolation width of 1.5 and subsequently fragmented with stepped normalized collision energy of 20, 30, and 40. The MS2 data was collected at 17,500 resolution with a maximum injection time of 100 ms, 1 microscan, and an automatic gain control target of $5x10^5$.

Supplementary Note 3: FBMN makes it possible to achieve relative quantification

Sample Preparation. The NIST SRM-1950 was prepared and extracted with 80% ethanol as proposed in the SRM 1950 paper[2].

Mass Spectrometry Analysis. The SRM1950 sample was analyzed using an ultra-high pressure liquid chromatography system (Vanquish, Thermo Fisher Scientific, MA, USA) coupled to an Orbitrap mass spectrometer (Q Exactive, Thermo Fisher Scientific, MA, USA) fitted with a heated electrospray ionization (HESI-II) probe. Chromatographic separation was accomplished using a Kinetex C_{18} 1.3 µm, 100 Å, 2.1 mm x 50 mm column fitted with a C18 guard cartridge (Phenomenex) with a flow rate of 0.5 mL/min. 5 µL of extract was injected per sample/QC. The column compartment and autosampler were held at 40°C and 4°C respectively throughout all runs. Mobile phase composition was: A, LC-MS grade water with 0.1 % formic acid (v/v) and B, LC-MS grade acetonitrile with 0.1 % formic acid (v/v). The chromatographic elution gradient was: 0.0 - 1.0 min, 5% B; 1.0 - 9.0 min, 100% B; 9.0 - 11.0 min, 100% B; 11.0 - 11.5 min, 5% B; and 11.5 - 12.5 min, 5% B. Heated electrospray ionization parameters were: spray voltage, 3.5 kV; capillary temperature, 380.0 °C; sheath gas flow rate, 60.0 (arb. units); auxiliary gas flow rate, 20.0 (a. u.); auxiliary gas heater temperature, 300.0 °C; and S-lens RF, 60 (arb. units). MS data was acquired in positive mode using a data dependent method with a

resolution of 35,000 in MS1 and a resolution of 17,000 in MS2. An MS1 scan from 100-1500 m/z was followed by an MS2 scan, using collision induced dissociation, of the five most abundant ions from the prior MS1 scan.

Data interpretation. Classical molecular networking does not use "area under the curve" the relative quantitative information obtained through feature detection of LC-MS traces. The FBMN method brings in ion abundance across all samples by using the value of chromatographic peak areas or peak heights as determined by the LC-MS feature finding software. Using a serial dilution of the NIST 1950 serum reference metabolome sample[2] analyzed on a Orbitrap instrument (3 LC-MS^2 independent experiments per sample) and process with MZmine or OpenMS, we show the linearity of the relative quantification capability with FBMN and reveals the improvement compared to classical molecular networking. As mentioned above, the most important limitation of classical molecular networking is the lack of dependable relative quantitative information. The interpretation of non-targeted LC-MS data in metabolomics relies on the statistical analysis of relative variation between ions intensity across the studied samples[3]. Classical molecular networking uses MS-Cluster results to define the ion distribution between the samples, using either the number of scans clustered in a consensus MS^2 spectrum (MS^2 scan table) or the sum of their precursor ion(s) intensities (MS^2 bucket table). A more accurate comparison of LC-MS data requires the value of chromatographic peak areas (EIC feature) or peak height for each ion features detected and aligned across the samples studied. The FBMN method makes possible to determine the relative intensity of each node in all samples. Using a serial dilution of the NIST 1950 serum reference metabolome sample analyzed on a Q Exactive mass spectrometer[4], we compared the capability of classical molecular networking and FBMN to evaluate the expected relative ion abundance. After basic optimisation of the software parameters, and as expected for serial dilution, the use of MZmine and OpenMS resulted in feature intensities with high coefficient of determination (R^2) values in Ordinary least squares Linear Regression (OLR) analysis for true positive compounds in the serial dilution samples with a mean R^2 of 0.92 (MZmine, (Figure 2g) and 0.71 (OpenMS, Supplementary Figure 13 and 14), respectively. These differences observed between MZmine and OpenMS processing are partially explained by 1) the lack of a gap-filling step with OpenMS which results in less features detected at the lower concentration range, along with 2) other differences due to the algorithms and parameters used. However, most importantly, the results of classical molecular networking showed that neither the number of MS^2 scans, or the sum of precursor ion intensity, were able to obtain acceptable coefficient of determination (R^2 mean 0.40 and 0.43, respectively, Supplementary Figures 15 and 17) for all the nodes and the reference compounds (R^2 mean 0.43 and 0.65, respectively, Supplementary Figures 16 and 18). The distribution of the R^2 value showed that ~50% of the features/nodes had a value of 0.33 both using the number of scans (Supplementary Figure 15) or the sum of the precursor ion intensity (Supplementary Figure 17), respectively. The prevalence of that value in both metrics can be explained by the prevalence of ions/features being selected for MS^2 scans in the most concentrated samples, but not in less concentrated samples. This shows that, while classical molecular networking can be used for

qualitative analysis, and that using the precursor ion intensity appears to perform better than the scan count, it is not suited for accurate ion intensity statistical analysis and that binary metrics (presence/absence) might be better suited to use. Nevertheless, binary interpretation of classical molecular networking should also be considered with caution, as the absence of MS^2 spectra for a compound in one sample does not necessarily mean that the compound was not present, rather than simply below the signal threshold in order to selected for MS^2 in data-dependent acquisition (DDA) or absent due to other reasons.

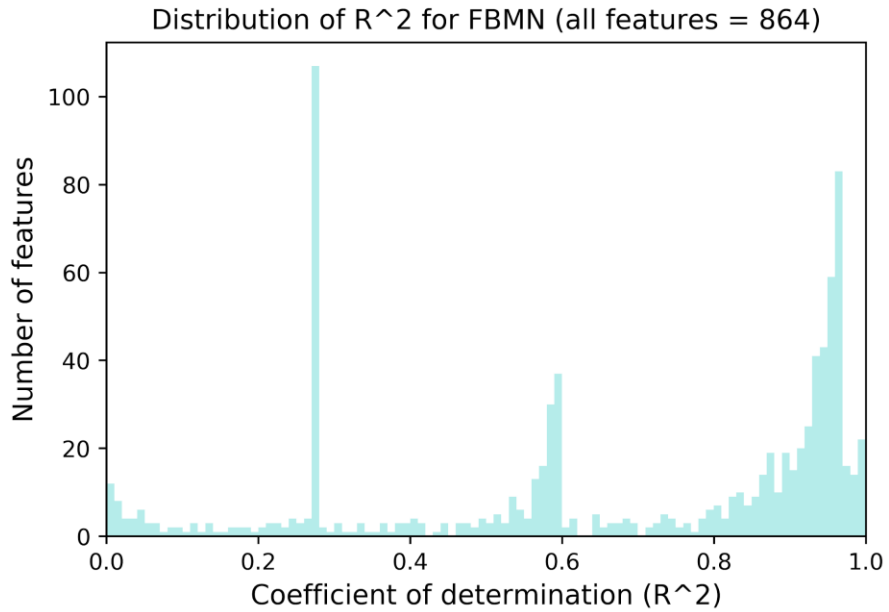

Supplementary Figure 13. Distribution of the coefficient of determination (R^2) from least square regression analysis between the feature intensities (n = 864) and the expected relative concentration for a serial dilution analyzed by LC-MS^2 (3 independent experiments per sample) and process with OpenMS for FBMN.

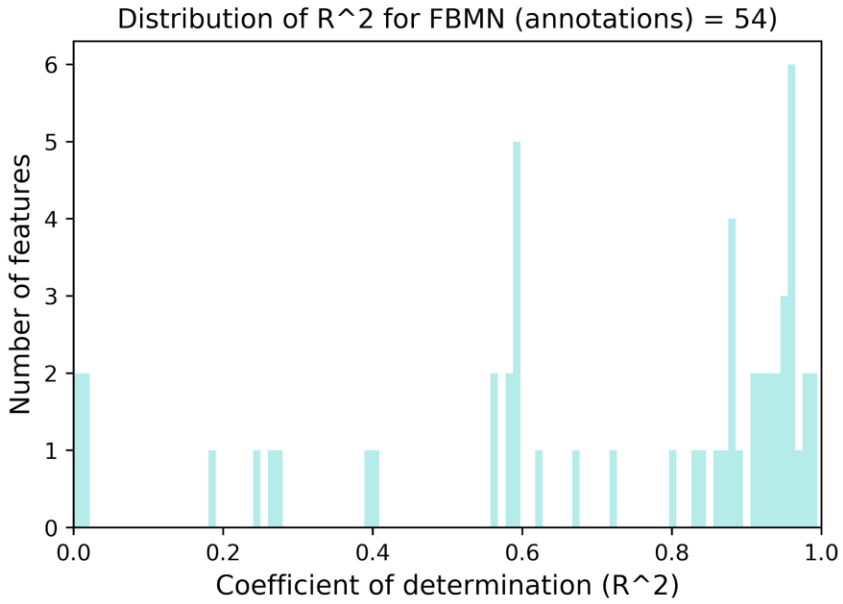

Supplementary Figure 14. Distribution of the coefficient of determination (R^2) from least square regression analysis between the feature intensities of annotated compounds (n = 54) and the expected relative concentration for a serial dilution analyzed by LC-MS^2 (3 independent experiments per sample) and process with OpenMS for FBMN.

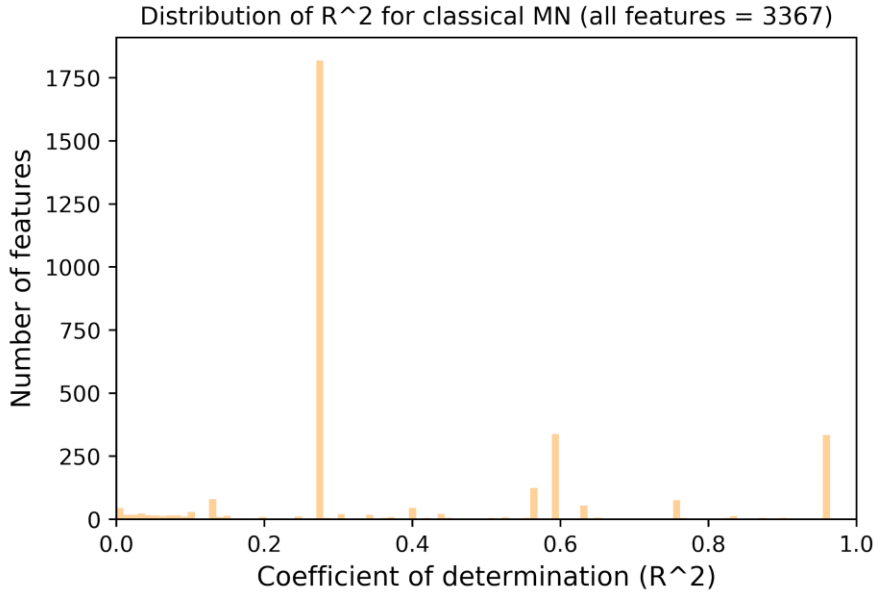

Supplementary Figure 15. Distribution of the coefficient of determination (R^2) from least square regression analysis between the feature (node, n =3,367) spectral count and the expected relative concentration with classical MN for a serial dilution analyzed by LC-MS^2 (3 independent experiments per sample).

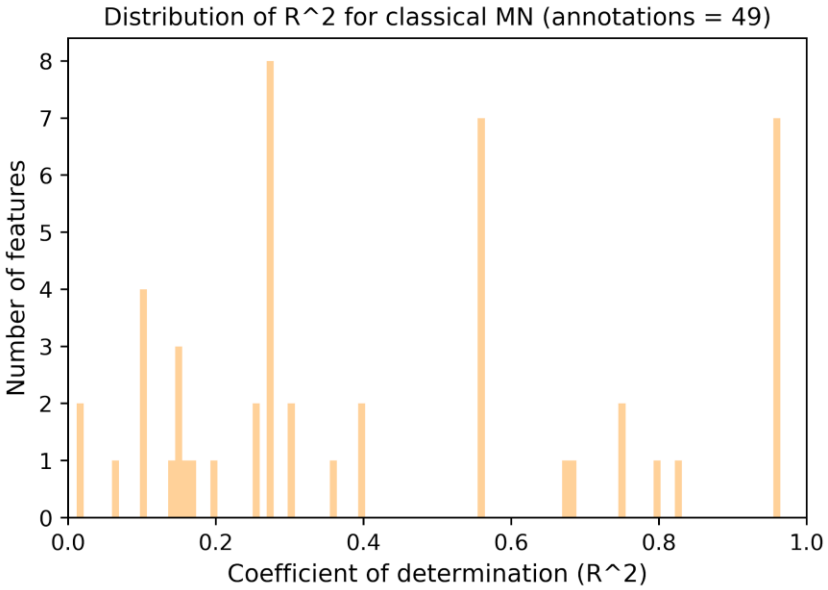

Supplementary Figure 16. Distribution of the coefficient of determination (R^2) from least square regression analysis between the feature (node) spectral counts of annotated compounds (n = 49) and the expected relative concentration with classical MN for a serial dilution analyzed by LC-MS^2 (3 independent experiments per sample).

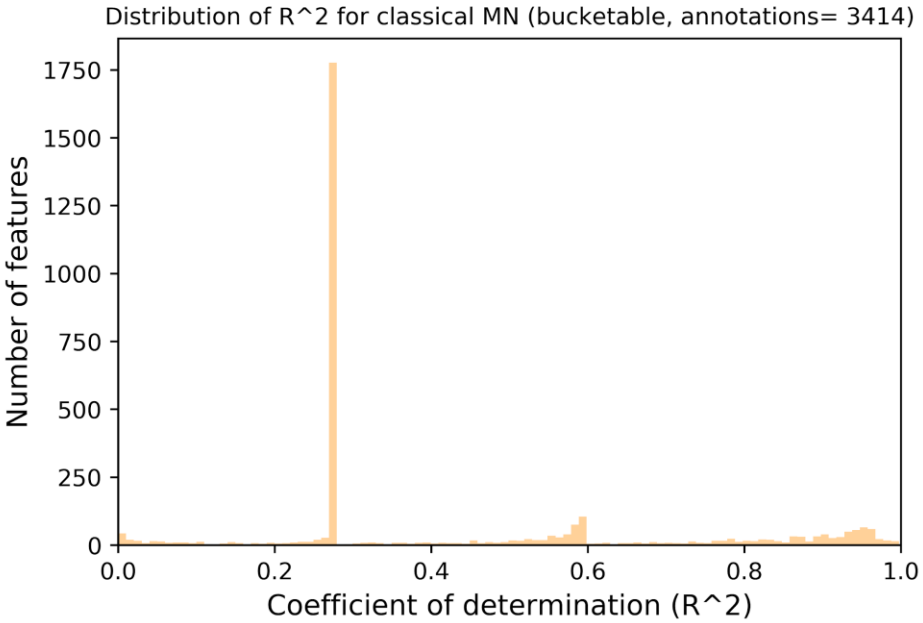

Supplementary Figure 17. Distribution of the coefficient of determination (R^2) from least square regression analysis between the feature (nodes, n =3,414) precursor intensity and the expected relative concentration with classical MN for a serial dilution analyzed by LC-MS^2 (3 independent experiments per sample).

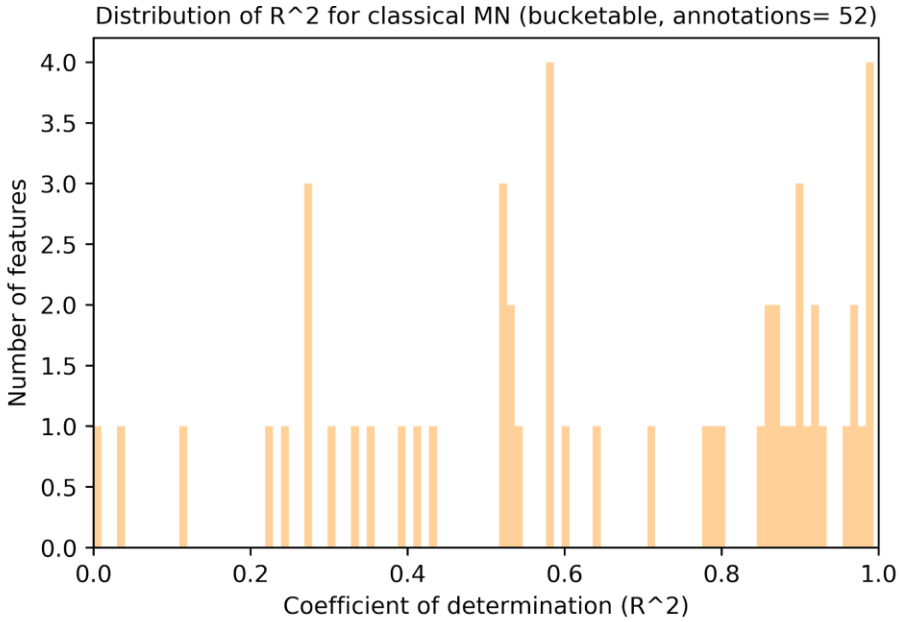

Supplementary Figure 18. Distribution of the coefficient of determination (R^2) from least square regression analysis between the precursor intensity for the annotated compounds (node, n

= 52) and the expected relative concentration with classical MN for a serial dilution analyzed by LC-MS^2 (3 independent experiments per sample).

Supplementary Note 4: Large dataset processing with XCMS

The processing of very large metabolomics dataset (more than a thousand samples) is limited by the scalability of existing LC-MS feature detection tools, especially for those based on graphical user interfaces (such as MZmine and MS-DIAL). MZmine was successfully used for the processing of large datasets acquired on QTOF mass spectrometers, but required both a powerful workstation computer (with 64GB of RAM memory), and the use of sub-optimal parameters, such as higher noise thresholds, to reduce the computational load. Here, we show that XCMS and OpenMS can be used to process large metabolomics studies for FBMN analysis. The MassIVE dataset MSV000080030 consists of approximately 2,000 samples from the forensic study with samples from hands and objects of 80 participants analyzed on a QTOF by LC-MS^2 [5]. The files were processed with XCMS or OpenMS running on cluster computers. For XCMS, the processing was performed on 8 processors with 32 GB of RAM memory allocated for each process and took 8 hours. The XCMS script is available at https://github.com/DorresteinLaboratory/XCMS3_FeatureBasedMN and the FBMN job on GNPS (https://gnps.ucsd.edu/ProteoSAFe/status.jsp?task=cf026a37c70946a1a937e030dea65514, runtime = 6 hours and 20 minutes).

For OpenMS processing, the OpenMS-GNPS workflow was used and run on the CCMS cluster (https://gnps.ucsd.edu/ProteoSAFe/status.jsp?task=e0a0694c3bcb42969d59354a822f5254#, runtime = 6 hours and 26 minutes). As observed for FBMN with XCMS, the number of features detected and spectral library matches show that, for large datasets FBMN will result in less annotations (0.7% instead of 1.0% for classical molecular networking, in Supplementary Table 2). Indeed, these feature detection tools were not designed to process multi-thousands files datasets. As a result, the processing of 2,000 files requires sub-optimal parameters (noise level, feature intensity threshold) to limit the computational load, and of heuristic(s) (such as a minimum number of occurrences in the dataset, or the presence of isotopologues) to limit the number of features outputted for downstream analysis. This illustrates the continued need for improvement of LC-MS feature detection on large metabolomics datasets, that will enable sensitive detection within a reasonable runtime.

Supplementary Table 2. Comparison of the results for the MassIVE MSV000080030 dataset (QTOF) including 2000 samples using classical molecular networking and feature-based molecular networking with XCMS.

	Number of features	**Single nodes**	**Unique library annotations**	**Spectral annotation rate**	**Runtime for feature detection/alignement**	**Runtime for molecular**

						networking on GNPS
Classical molecular networking	20,578 (nodes)	18,946 (92,1%)	208	1.0 %	Not applicable	11h44min
Feature-based molecular networking with XCMS	13,862 (LC-MS features with MS2)	12,045 (86.9%)	97	0.7 %	6h26min	6h20min

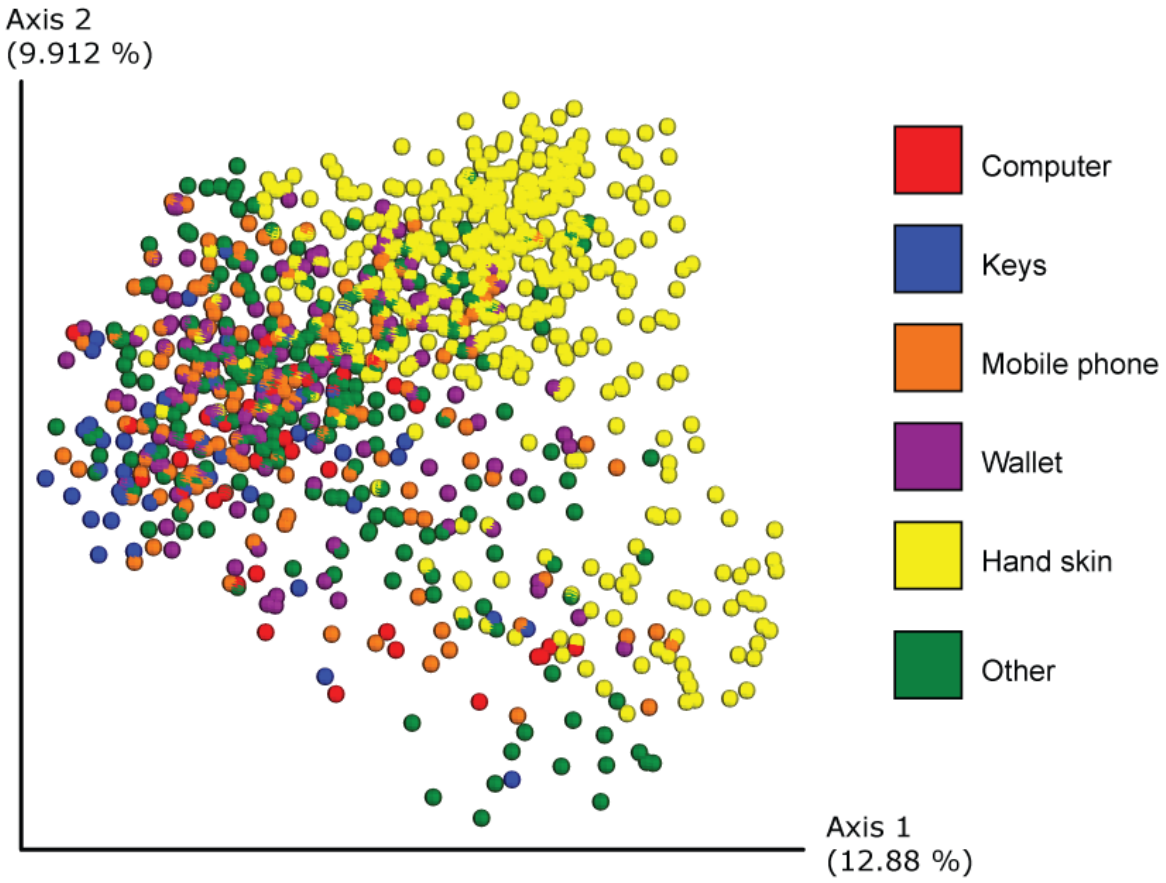

Supplementary Figure 19. Principal Coordinate Analysis of the forensic study (MSV000080030, approximatively 2,000 samples, n= 1 LC-MS^2 experiment per sample) processed with XCMS and analyzed with the FBMN workflow on GNPS. See this link for an interactive visualization of the plot.

References for Supplementary Information

1. Nothias, L.-F. *et al.* Bioactivity-Based Molecular Networking for the Discovery of Drug Leads in Natural Product Bioassay-Guided Fractionation. *J. Nat. Prod.* **81**, 758–767 (2018).
2. Simón-Manso, Y. *et al.* Metabolite profiling of a NIST Standard Reference Material for human plasma (SRM 1950): GC-MS, LC-MS, NMR, and clinical laboratory analyses, libraries, and web-based resources. *Anal. Chem.* **85**, 11725–11731 (2013).
3. Sugimoto, M., Kawakami, M., Robert, M., Soga, T. & Tomita, M. Bioinformatics Tools for Mass Spectroscopy-Based Metabolomic Data Processing and Analysis. *Curr. Bioinform.* **7**, 96–108 (2012).
4. da Silva, R. R. *et al.* Computational Removal of Undesired Mass Spectral Features Possessing Repeat Units via a Kendrick Mass Filter. *J. Am. Soc. Mass Spectrom.* **30**, 268–277 (2019).
5. Bouslimani, A. *et al.* Lifestyle chemistries from phones for individual profiling. *Proc. Natl. Acad. Sci. U. S. A.* **113**, E7645–E7654 (2016).